EFFECTS OF MICROWAVE ENERGY TREATEMENT ON VALUE LIBERATION FROM Zn AND Co-Cu ORES

Antoine F Mulaba – Bafubiandi and John M L Lewis

Abstract

In the irradiation of ore particles by microwave energy preferential absorption of this energy occurs in minerals having specific dielectric properties (Bradshaw, 1999). This leads to a selective heating of the various components of within the ore particle matrix. The result is a differential thermal expansion of such components and the resulting induced stresses become ideally concentrated at mineral grain boundaries (Kingman et al., 2000). Dependent upon the relative composition of absorbent, opaque and reflective components this may lead to enhancement of the inter-granular fracture of the ore particles in the initial comminution process (Fandrich et al., 1997). The potential is thus a greater proportion of free mineral grain within the fractured ore particle that may lead to improvement in subsequent mineral separation processes. As the composition of the ore dictates the result of such a treatment (Kingman et al., 2000) it is essential to evaluate the response of each ore sample on an individual basis. This paper reports on results obtained from two ore samples: the one being the zinc ore from the Black Mountain mine (South Africa) and the other a pre-concentrated sample of handpicked cobalt–copper mixed oxide ore from the Gecamines (DRC). The equipment and methods used to simulate the comminution of the samples and evaluate the level of the value liberation will be described along with the results obtained. Using King (1975), Kanellopoulous and Ball (1975), and Gungor and Atalay (1998), a comparison between the behaviour upon microwave irradiation of sulphide and mixed oxide ores leads to conclude that while the technique (i.e. microwave irradiation) is appropriate to the zinc sulphide ore, it does not seem to lead to exceptional results for the oxide.

1. Introduction

The effect upon ores of microwave irradiation includes the heating by means of energy transfer from the wave in addition to a possible reaction or phase transformation within the material. The principle of generalised heating of ore particles both to reduce the energy required in comminution has long been acknowledged but has not been proved to the economic in practice. This as a consequence the thermal energy requirements to heat the total material being in excess of the energy saved in the comminution process.

When the effect of heat prior to comminution is considered from the aspect of mineral liberation Geller and Tervo (1975) noted that mineral grains were liberated at coarser sizes follow a sequence of heating and quenching when compared to conventional comminution treatment and also cited the findings of Brown, Gaudin and Loeb (1958) on liberation of Feldspar from Granite, these investigations focusing upon the milling aspect of comminution.

Investigations by Kanellopoulos and Ball (1975) demonstrated the reduction in strength under compressive forces of quartzite materials heated beyond the α to β phase transition temperature. They noted that stresses could be produced by both volume changes and anisotropic thermal expansion.

The advantage to be gained from microwave energy is to generate a differential heating of the various components comprising the ore particle matrix as a consequence of the difference in dielectric properties of the mineral components in the ore particle matrix. This in turn leads the development of internal stresses through differential thermal expansion of the components within the particle holding the prospect of improved mineral liberation at lower energy requirements.

Due to the known limitations in power availability in the domestic microwave oven used in this investigation single particle treatment was indicated and it was decided to study the effect in relation to crushing under conditions where compressive stress was emphasized as per Kingman and Bradshaw (1998). The development of the equipment for this was carried out on the zinc sulphide ore sample.

2. Background on microwave assisted value liberation

A more comprehensive coverage on the use of microwaves in minerals processing is found in the literature (Kingman and Rowson (1998), Patnaik and Rao (2004) and Bradshaw (1999)).

The effects that microwave irradiation have upon the ores investigated are induced as a consequence of the energy transfer between the microwaves and the mineral species present.

The effects on the minerals result from the differences in their dielectric properties. As with any energy form microwaves may be absorbed, reflected or transmitted by materials. When they are absorbed the internal dipoles of the structure attempt to align with the fluctuating magnetic field of the wave. Due to the high frequency of the waves this attempted alignment results in rapid vibration of such dipoles creating internal friction within the structure that in turn leads to the generation of heat. This heat then results through internal heat transfer into thermal expansion of the absorbent materials, the reflective and opaque components being affected to significantly lesser extent. The result of this differential heating being the generation of internal stresses as a consequence of alteration in the dimensions of components within the ore particle matrix. The internal stresses should consequently be maximised at mineral grain boundaries. Such stresses can therefore result in decrease in the cohesive strength of the particle. As the stresses are focused at mineral grain boundaries, when external forces are applied to disrupt the

particle matrix, fragmentation should occur preferentially at such boundaries holding the prospect of improved free mineral grain liberation.

The magnitude of the developed stresses is a function the composition of the material under investigation. Composition in this context relating to the following components: Mineral species present (opaque, reflective, absorbent), their grain size and proportionate dispersion through the particle matrix. Thus whilst the principles are generally accepted and some work has been reported on numerical modeling of particle breakage taking these factors into account, Whittles et. al (2003) and other investigators e.g. Gungor and Atalay (1998) found the energy absorbance of the species present in their test materials inadequate to generate a reduction in the measured breakage. It is thus suggested that each ore sample must be examined and evaluated on its individual response to such processing.

3. Experimental

3.1. Materials

Two dissimilar materials one a sulphide and the other an oxide both of African origin, one of which is from a current production operation within RSA, the other from the DRC not currently commercially exploited are reported upon.

3.1.1. The sulphide sample.

This is derived from the Black Mountain sulphide ore body currently exploited in the Northern Cape and has been in operation for a number of years producing by means of a flotation process concentrates containing lead (Pb), zinc (Zn) and copper (Cu). Its mineralogy and genesis are described in Beck and Chamart (1980). The mineralogy of the sample material was confirmed by XRD analysis of selected specimens the results of which are shown in section 4.

3.1.2. The high grade cobalt oxide sample.

This is a handpicked pre-concentrated material, extremely high grade imported in the country for further commercial transactions. Its mineralogical composition was determined by stereo-optical microscopy and XRD examination the results of which are shown in section 4.

3.2. Methodology / Techniques employed.

One of the first aspects to consider is how to assess the mineral or value liberation. This boils down to firstly identify what the effect of conventional crushing has upon this factor before attempting to evaluate the effects of the microwave irradiation.

As the comminution process is designed to reduce the size of particles in order to liberate the particle components for processing, determination of particle size distribution prior to and post irradiation is of significance. This is carried out using standard screen analysis equipment in the form of calibrated screens and a sieve shaker.

The actual particle breakage aspect of this has been handled in two ways: The zinc sulphide ore sample was conventionally crushed through three stages of laboratory comminution equipment in the form of Jaw, Roll and Cone crushers to 100% less than 4 mm to provide a reference sample Particle Size Distribution (PSD) suitable for application of the value separation processes to be used for evaluation of the effects of the microwave irradiation.

As the high grade cobalt oxide sample (~n30 % Co) already presented a wide PSD such treatment was not required in this case.

The microwave equipment used was a 900 W, 2.45 GHz, multimode cavity. It was thus considered that treatment of single particles of up to 50 mm screen size was the only feasible solution to this limitation.

This then required the identification of a comminution technique for handling single particle breakage under the desired compressive loading. The basic design of the crushing chamber is detailed somewhere else (Lewis, 2005) and the development of the technique and the equipment used is described as follows.

This comprises basically two components, the one item comprising the various compression chamber elements containing the sample materials and the other being the mechanism used to apply and control the rate of loading. The compression chamber components were fabricated from BMS in the basic form of cylindrical pistons and anvils.

For single particle tests the cylindrical components were machined with an internal clearance of 0.5 mm to fit neatly within a 50mm internal diameter (ID) steel pipe section that contained the fragments generated.

A variety of profiles for both anvil and piston faces were tested to locate the particles which had irregular shapes as near as feasible with the centre line of the piston.

For testing of packed bed particles a piston and cup with an ID of 80mm and wall thickness of 5mm were machined from BMS to match. The piston was fitted with a 40 mm shaft treaded into the centre of the piston and was machined to give a clearance of 200microns relative to the internal diameter of the cup.

Both the shaft of the cup design and the piston of the single particle test unit had a recess machined to take a ball used for connection to the loading test unit.

The equipment used to apply the load to the sample materials were standard units of California Ball Ratio (CBR) used for the testing of building materials (concrete and soil).

The equipment identified was in the form of a load frame of the form used in the standard CBR (California Ball Ratio) test as used for concrete and soil tests.

The one unit had a load frame capacity of 50kN, a load cell of capacity of 100 kN and a mechanical drive. The load cell is fitted with a transducer linked to the software programme controlling the rate of travel, displacement and load measurement limit to within the capacity of the load frame.

The other unit had a load frame capacity of 200 kN and was driven hydraulically under control of the same software programme.

The basic programmed parameters used were as per a standard CBR with the rate of piston displacement set at 1.27mm/min and a displacement limit of 10mm. On the mechanically driven unit a load limit of 40kN was also incorporated in the software programme to eliminate the risk of damage to the load frame.

The low rate of piston displacement was selected to generate conditions of slow compression and the displacement limit with the requirement of a small reduction ratio. These requirements being those regarded as an approach to ideality for compressive comminution.

To gain insights on the effects of microwave irradiation upon value distribution in addition to that of fragmentation selected size interval fractions from both original and product PSD’s were partitioned with a heavy liquid. The liquid selected was Tetrabromoethane with a density of 2.95. It is recognized that this may not be a suitable density to partition the heavy minerals but would prove adequate for gangue minerals separation from the value bearing constituents of the particle matrix. This however is not the only motivation for the selection as factors such as cost and availability are also significant and the use of heavier solutions such as those generated with the use of Thallium salts were discounted on the basis of toxicity.

As the valuable minerals identified within the sample materials are all of relatively high density the measurement of densities on particles was also applied within the various testing procedures. Coarse particles densities being determined by a simple wet volumetric displacement technique and finer fraction with the use of a micrometrics multi-volume Pyknometer model 1305.

Analytical techniques in the form of acid digestion and Atomic Absorption Spectrometry (AAS) were used for elemental determination upon the high grade cobalt sample and carbonate peroxide fusion followed by AAS used for the Black Mountain sample. XRF was additionally used on selected samples.

4. Results and Discussion.

4.1. Zinc bearing sulphide ore.

Based on their apparent weights, two specimens selected from the coarse material of the zinc sulphide bearing ore (Black Mountain ore) were examined by means of XRD. The identification of the major mineral contents was found to be in agreement with the literature (Beck and Chamant, 1980), Table 1, revealed that the material with a higher density (4.11) showed the anticipated heavy minerals content whilst the one with the lower density (2.73) comprises mainly gangue minerals. The content of the high density sample material comprise, quartz, galena, pyrite, magnetite, sphalerite and pyrrhotite and that of the low density sample being Quartz, muscovite, microcline and clinochlore. The samples were additionally analysed for their elemental contents by both AAS and XRF.

Table 1: Identification of major mineral contents in the zinc sulphide ore sample

Sample	**Density**		**AAS**		**XRD**				**XRF**		
		% Cu	% Pb	% Zn			% Cu	% Pb	% Zn	% SiO_2	% Al_2O_3
Light	2.73	0.57	2.18	0.46	Quartz, muscovite, microcline and clinochlore		0.61	1.14	0.2	60.5	17.4
Heavy	4.11	0.70	37.30	2.50	Quartz, galena, pyrite, magnetite, sphalerite and pyrrothite		0.39	30.40	3.70	26.30	1.50

Whilst the figures from AAS and XRF analytical techniques are not identical, they nevertheless give confirmation of the composition and value distribution. The PSD of the crushed Black Mountain sample used for reference purposes is shown in table 2 below.

Table 2: Particle Size Distribution of the crushed zinc sulphide ore

Size mm	% mass	Cum % mass Pass	Cum % mass Ret.	Size mm	% mass	Cum % mass Pass	Cum % mass Ret.
4	6	94.2	6	0.355	1.5	13.1	87.1
2.8	19	75.2	25	0.3	1.7	11.4	88.8
2	24.9	50.3	49.9	0.212	2.4	9	91.2
1.4	14.7	35.6	64.6	0.15	2.2	6.8	93.4
1	8.4	27.2	73	0.106	1.8	5	95.2
0.85	3.4	23.8	76.4	0.075	1.3	3.7	96.5
0.71	2.6	21.2	79	0.053	0.9	2.8	97.4
0.6	2.4	18.8	81.4	0.038	0.8	2	98.2
0.5	2.6	16.2	84	-0.038	2		
0.425	1.6	14.6	85.6		100.2		

The graphical representation of this data is shown in figure 1 and the value of the correlation coefficient against linearity confirms that this distribution conforms to that which is conventionally anticipated from a crushing comminution operation.

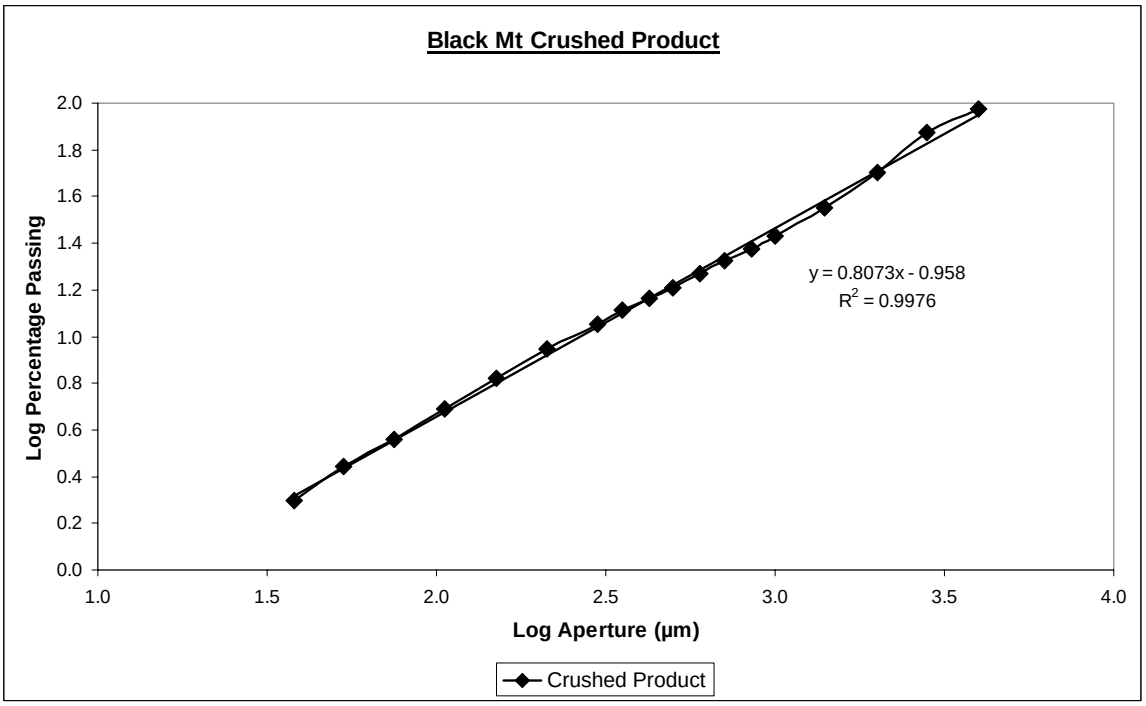

Figure 1: Particle Size Distribution of the crushed zinc sulphide ore.

The particle size range intervals selected for the heavy liquid separation were those within which the particles would settle rapidly under a standard gravitational field only the ranges coarser than 500µm were tested. As each size range interval will contain particles of varying composition it is assumed that those composed of predominantly gangue minerals would float at the density selected for the separation. However to evaluate the effect of density separation some indication of the initial value content of the size range interval is considered to be valuable information in such an evaluation. Thus the size range intervals between 2000µm and 500µm were analysed for their elemental content. The results for these determinations are shown in table 2.

Along with these determinations the densities of the size interval contents were measured on the Pyknometer using the 5ml cell.

Here it can be seen that the densities of the various fractions are very similar as would be anticipated on the basis of the similarity of the analyses. This absence of any discernable trends being anticipated when the errors in both the analyses and the density determinations are considered. Having the initial densities and the analyses for these size fraction intervals the investigation proceeds to identify what composition variations may be identified within them based upon a density difference by partitioning with the heavy liquid, Table 3.

Table 3: Size fraction interval densities and elemental (AAS) analysis of conventionally crushed zinc sulphide ore fines. Mass partitioning is there added.

Size mm	Density	%Cu	%Pb	%Zn	% mass sink	Density sink	% mass float	Density float
2	3.23	0.53	4.62	0.88	44.0	3.84	56.0	2.72
1.4	3.38	0.42	1.89	1.13	50.9	4	49.1	2.75
1	3.47	0.4	0.93	1.06	53.4	4	46.6	2.81
0.85	3.45	0.35	0.75	0.77	54.3	4.1	45.7	2.74
0.71	3.48	0.37	1.58	0.75	51.1	4.2	48.9	2.72
0.6	3.36	0..32	1.33	0.78	52.9	4.3	47.1	2.87
0.5	3.36	0.38	1.47	0.83	51.0	4.3	49.4	2.76

As expected a significant density difference is observed between the float fraction materials and those that sink. It is also evident that they are both different to the values determined for the composite contents of the corresponding size interval fractions and also to the liquid density used in the separation. These differences become even more evident when the data is presented in a graphical format as shown in figure 2.

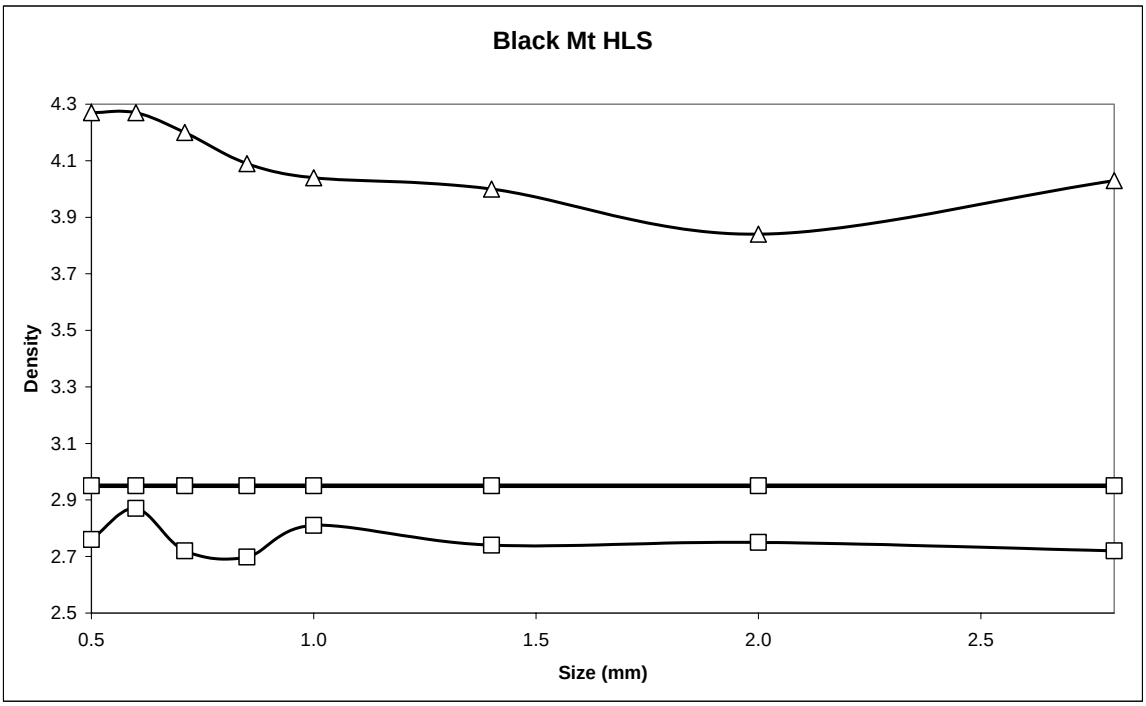

Figure 2: Heavy Liquid Separation curve for the zinc sulphide ore

The differences in density between the product and the partitioning density are less pronounced for the float materials than the sink products, possibly due to the proximity of gangue mineral densities to the partitioning density. This will depend upon the relative content of the various minerals present in the specific sample as the densities of the components identified by XRD are clinochlore (2.75), muscovite (2.93) and quartz (2.65).

An attempt to interpret this difference in density in terms of value content lead to the analysis of the float products for their elemental content and the following results obtained as shown in table 4.

Table 4: Analysis of float fractions from zinc sulphide ore

Size microns	% Cu	% Pb	% Zn
2000	0.07	0.07	0.18
1400	0.02	0.13	0.29
1000	0.02	0.12	0.38
850	0.01	0.10	0.31
710	0.02	0.15	0.28

It is seen that as anticipated the heavy mineral content of these fractions is low based upon the above analyses.

Here it may be appropriate to consider in more detail the relation between density and the mineral content. If we examine the analytical results for the coarse sample materials shown in tables 1 and 2 and translate these into mineral content of the major components identified by XRD on the basis of the elemental content of the mineral compositions, a semi quantitative estimate of the respective mineral content of the particle can be made. From the known physical properties of the minerals specifically their densities an estimate can be made for the density of the composite particle. The details of this procedure are shown in the following examples related to the samples identified in tables 1 and 2.

In the high density sample the following minerals are identified galena, sphalerite, chalcopyrite and quartz. The elemental composition of these is taken to be galena (PbS), sphalerite (ZnS), chalcopyrite ($Cu_2S.Fe_2S_3$) and their respective densities as PbS (7.5), ZnS (4) and $Cu_2S.Fe_2S_3$ (4.2) the quartz density being taken as 2.65 and their elemental contents are respectively 86.6%Pb, 67.1% Zn and 34.8% Cu.

Taking the analytical values for the AAS the contents can be calculated as shown below.

% lead mineral = 27.3/0.866 = 31.5%

% zinc mineral = 2.54/0.671 = 3.8%

% copper mineral = 0.7/0.384 = 1.8%

% quartz by difference = 62.9%

From these % mass contents the composite density is calculated,

Composite density = 0.315 x 7.5 + 0038 x 4 + 0.018 x 4.2 +0.629 x 2.65 = 4.26.

The difference against the measured value is thus 0.15 units or as a % against the computed value 3.6%. Considering the crude method used for the original density determination this difference is insignificant. Using the XRF analysis in the same manner the density computed is 4.44 which is 7.4 % difference again considered as insignificant. When the figures for the lower density sample are considered, the results for the AAS figures generate a computed value of 2.81 against a measured value of 2.73 a % difference of 2.9% and with the XRF values computed 2.72 against measured 2.73 the difference here definitely being insignificant. It is therefore suggested that the use of density measurements can be a valid pre-assessment procedure to identify potential value liberation upon this sample material. The acceptance of this assumption will lead to a reduction in cost by selection of those materials upon which the more costly and time consuming techniques such as XRD and fusion analysis are to be applied.

The next stage was to evaluate the compression comminution technique and equipment performance upon the sample. As previously noted the testing of individual particles has been chosen as the appropriate method for the reasons given relating to power limitations of the microwave equipment. Using the equipment previously described a particle was tested and the results of the load versus displacement response are shown in tabular and graphical format following.

Table 5: Load versus displacement for a zinc sulphide ore sample.

Disp. mm	Load kN	Disp.mm	Load kN
0.64	1.01	5.72	9.96
1.27	4.92	6.35	10.74
1.91	6.15	6.99	15.66
2.54	11.86	7.62	14.65
3.18	17.11	8.26	17.9
3.81	13.2	8.89	7.27
4.45	15.80	9.3	9.96
5.08	8.95		

It is observed that particle fracture is taking place by increments as a consequence of the inherent flaws (micro cracks) yielding under the increasing stress applied. To compare

the fragmentation generated from this procedure with that anticipated from a crusher the products were taken for sieve analysis and the results are shown in table 6.

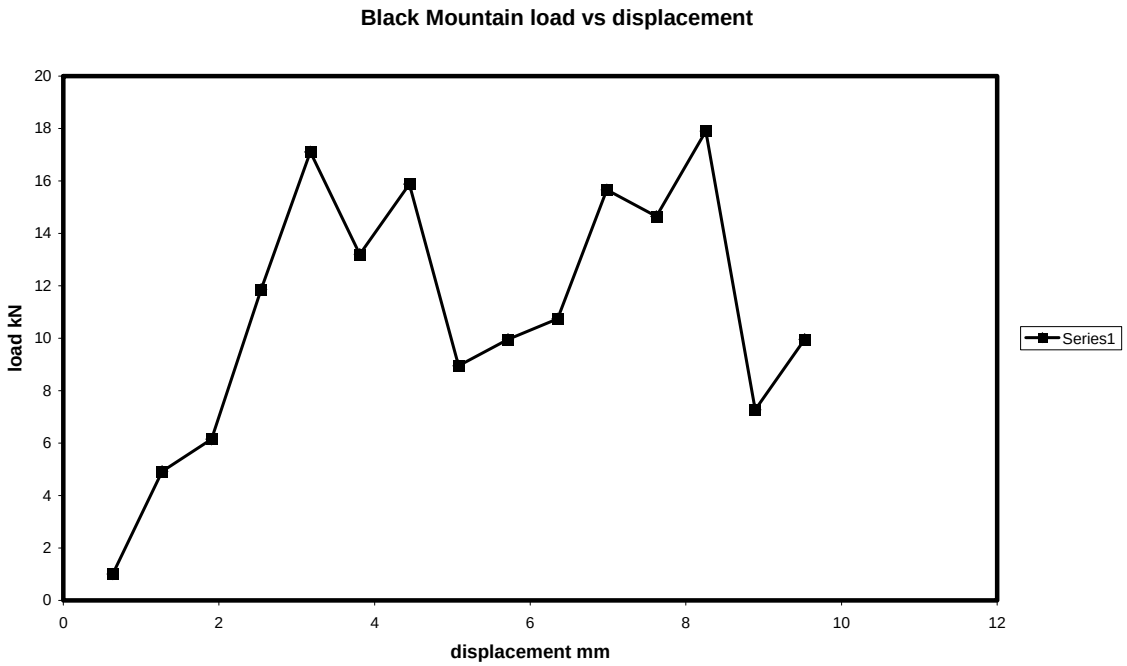

Figure 3: Load versus displacement in zinc sulphide ore

.

Table 6: Size grading of products from the compression test on the zinc sulphide ore.

Size mm	% mass retained
11.2	77.2
8	6.2
5.6	2.1
4	3.9
1.4	3.7
-1.4	6.9

To confirm that the distribution corresponds with that from a crushing application the data is plotted in figure 4. The approach to linearity of the plot confirms that the test was a fair simulation of a crushing environment. The linear correlation coefficient being 0.97 which considering the limited data base is reasonable.

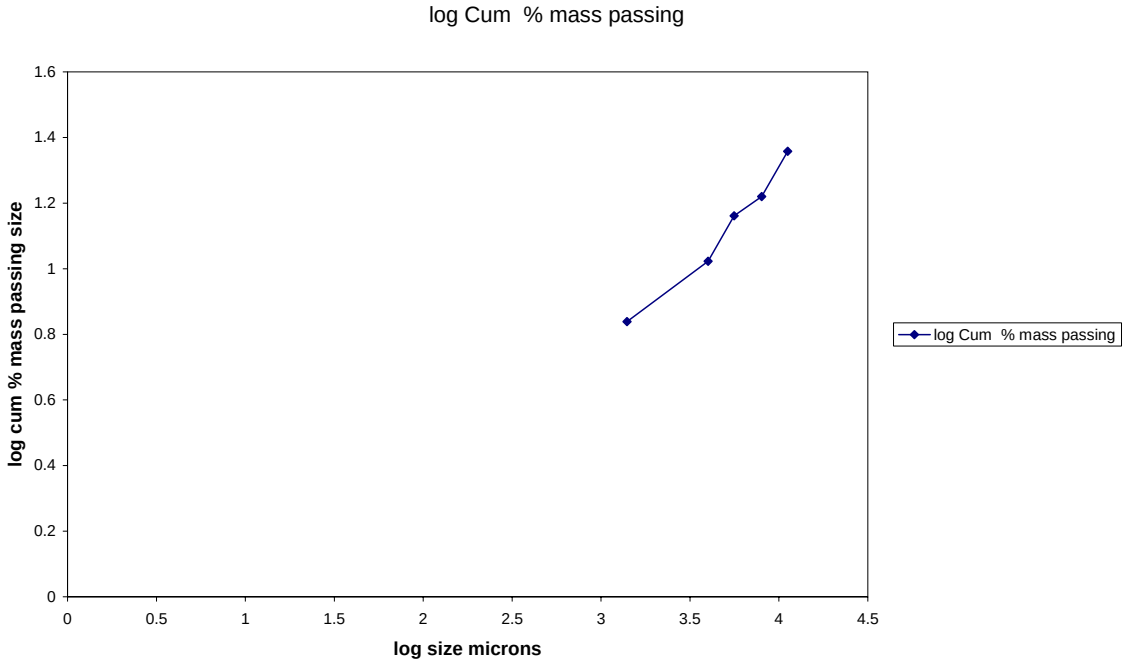

Figure 4: Product size distribution from compression test for the zinc sulphide ore.

To confirm this result and obtain a preliminary view of the effect of microwave irradiation upon this aspect of the investigation a number of coarse particles were selected and exposed to microwave irradiation prior to the compression test and their product gradings examined. Data relating to the particles irradiated is shown in table 7.

Table 7: Some measurements on particles used in microwave irradiation prior to compression.

Sample	Irradiation time secs	Maximum surface temp	Density	Mass gms
A22	0	18	3.53	77.7
A46	30	65	2.86	48.6
A49	60	150	4.24	63.6
A45	90	205	3.51	70.1
A33	90	231	3.72	137.8

It is observed that relatively short exposure times (up to 90 seconds) are effective in heating the particles even with the limited power available (900 W). The load versus displacement response for the particles listed in table 7 is shown in figure 5.

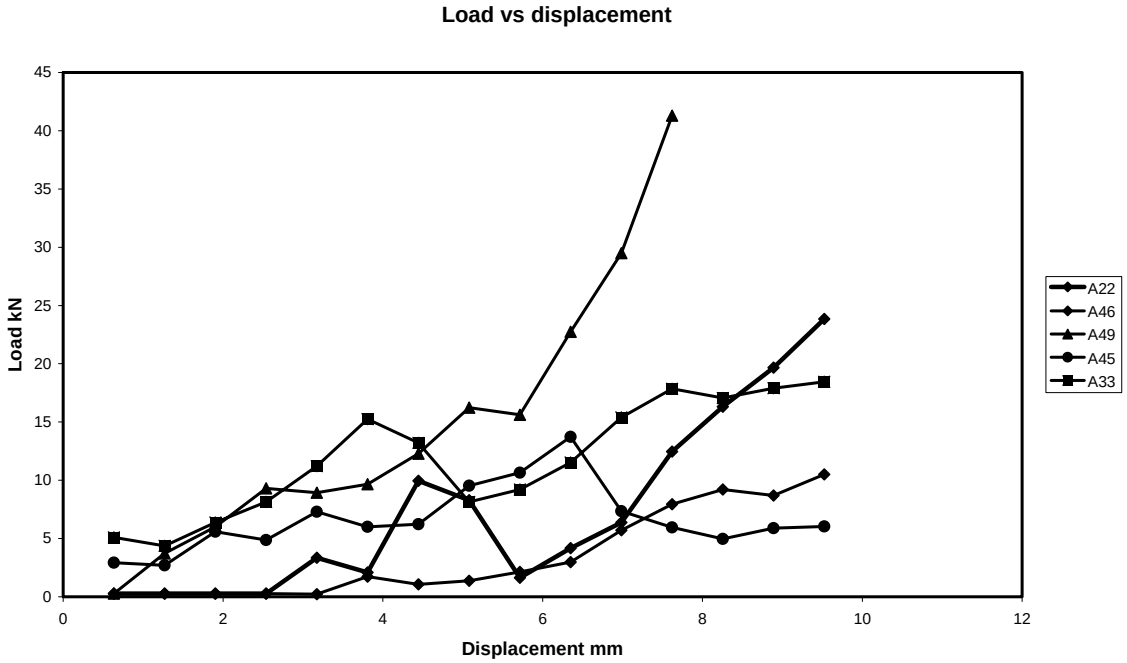

Figure 5: Load versus displacement response of particles in table 6

Although a complete critical evaluation of this data has not yet been conducted it is apparent that the non irradiated particle does not break as easily as those that have been microwaved, and even the highest mass particle breaks more easily. The resultant product size analysis is shown in table 8.

Table 8: Size analysis of compression tested samples from table 7.

Sample	% mass retained on 16 mm	% mass retained on 11.2 mm	% mass retained on 8.0 mm	% mass retained on 6.7 mm	% mass retained on 5.6 mm	% mass passing 5.6 mm
A22	28.0	15.2	17.5	3.9	4.4	30.9
A46	15.9	21.7	12.3	4.6	7.3	38.2
A49	13.4	8.8	12.8	5.4	6.3	53.3
A45	68.7	5.9	5.3	1.6	1.9	16.6
A33	70.9	7.8	2.2	1.8	3.0	14.3

A critical examination of this data is still to be undertaken but it is immediately apparent that the smallest % of – 5.6 mm is produced from the largest particle even though the greatest amount of fines are generated from the particle with the highest density. This may be a consequence of a greater content of microwave absorbing minerals which

cannot be identified from surface temperature measurements but may be inferred from the previous consideration of composition related to density.

4.2. Microwave assisted liberation of cobalt bearing minerals.

On the basis of the observations on the zinc sulphide ore that density can be a precursor indication of value content, density determinations were made upon coarse and fine particles from a cobalt-copper mixed oxide ore. It was observed that the sample material suggested low densities and was friable. In an attempt to identify competent particles suitable for the compression testing, it was decided to examine coarse particles generated from an attritioning process applied to coarse particles from the original sample. The product size grading from the attritioning test is shown in table 9 and both products shown graphically in figure 6. Coarse samples from the attritioned product were tested for their densities by the same simple wet displacement method. During this exercise it was observed that the particles were porous as evidenced by gaseous evolution during tests. 65 particles were tested in this manner and the average density found to be 2.57. Considering that the sample was of high grade (~30 % Co) and the cobalt mineral density is 4.32 such a value can only result as a consequence of porosity.

Table 8: Particle size distribution of original cobalt–copper mixed oxide ore sample.

Mesh mm	% Mass	Cum. % Mass Passing	Cum. % Mass Retained	Mesh mm	% Mass	Cum. % Mass Passing	Cum. % Mass Retained
40	20.35	79.63	20.35	0.85	0.63	12.42	87.56
25	37.14	42.49	57.49	0.71	1.07	11.35	88.63
19	11.05	31.44	68.54	0.6	0.55	10.8	89.18
14	1.53	29.91	70.07	0.5	0.88	9.92	90.06
11.2	4.70	25.21	74.77	0.425	0.52	9.4	90.58
8	2.18	23.03	76.95	0.355	0.57	8.83	91.15
6.7	0.93	22.1	77.88	0.3	0.74	8.09	91.89
5.6	1.18	20.92	79.06	0.212	1.07	7.02	92.96
4	1.63	19.29	80.69	0.15	1.32	5.7	94.28
3.35	0.68	18.61	81.37	0.106	0.93	4.77	95.21
2.8	0.92	17.69	82.29	0.075	0.58	4.19	95.79
2	1.55	16.14	83.84	0.053	0.77	3.42	96.56
1.4	1.60	14.54	85.44	0.038	1.10	2.32	97.66
1	1.49	13.05	86.93	-0.038	2.32		99.98

In an attempt to determine how far down the size range spectrum the porosity persisted, density determination measurements were made upon the fine sizes from the screening analysis or both the original sample and the attritioned product. Here the value for the 40 sample portions examined was generally in excess of 3.4. The particle size distributions determined for both the original sample and the attritioned material are shown in the following tables 8 and 9, and figure 6.

Table 9: Particle Size Distribution of attritioned cobalt bearing mixed oxide ore material

Mesh mm	% Mass	Cum. % Mass Passing	Cum. % Mass Retained	Mesh mm	% Mass	Cum. % Mass Passing	Cum. % Mass Retained
40	20.75	79.25	20.75	0.85	1.30	78.13	21.87
25	28.92	50.33	49.67	0.71	2.34	80.47	19.53
19	5.70	44.63	55.37	0.6	1.05	81.52	18.48
14	2.73	41.90	58.10	0.5	2.53	84.05	15.95
11.2	3.08	38.82	61.18	0.425	0.68	84.73	15.27
8	1.22	37.60	62.40	0.355	0.69	84.52	14.58
6.7	0.99	36.61	63.39	0.3	0.88	86.30	13.70
5.6	1.27	35.34	64.66	0.212	1.54	87.84	12.16
4	1.81	33.53	66.47	0.15	1.83	89.67	10.33
3.35	1.03	32.50	67.50	0.106	1.35	91.02	8.98
2.8	0.99	31.51	68.49	0.075	1.84	92.86	7.14
2	1.48	30.03	69.97	0.053	1.77	94.63	5.37
1.4	4.24	25.79	74.21	0.038	0.96	95.59	4.41
1	2.62	23.17	76.83	-0.038	4.41	100.00	

Apart from the earlier comments about low density and friability the format of this presentation draws attention to the unusual nature of this sample material. The format of presentation used for the above figure is that conventionally associated with materials that have been subjected to crushing comminution stage. That a sample reputedly to be hand picked should match such a format is to say the least anomalous and that the attritioned product should also conform to the same format suggests an ore that cannot be regarded as competent and of a different genesis from the sulphide ore.

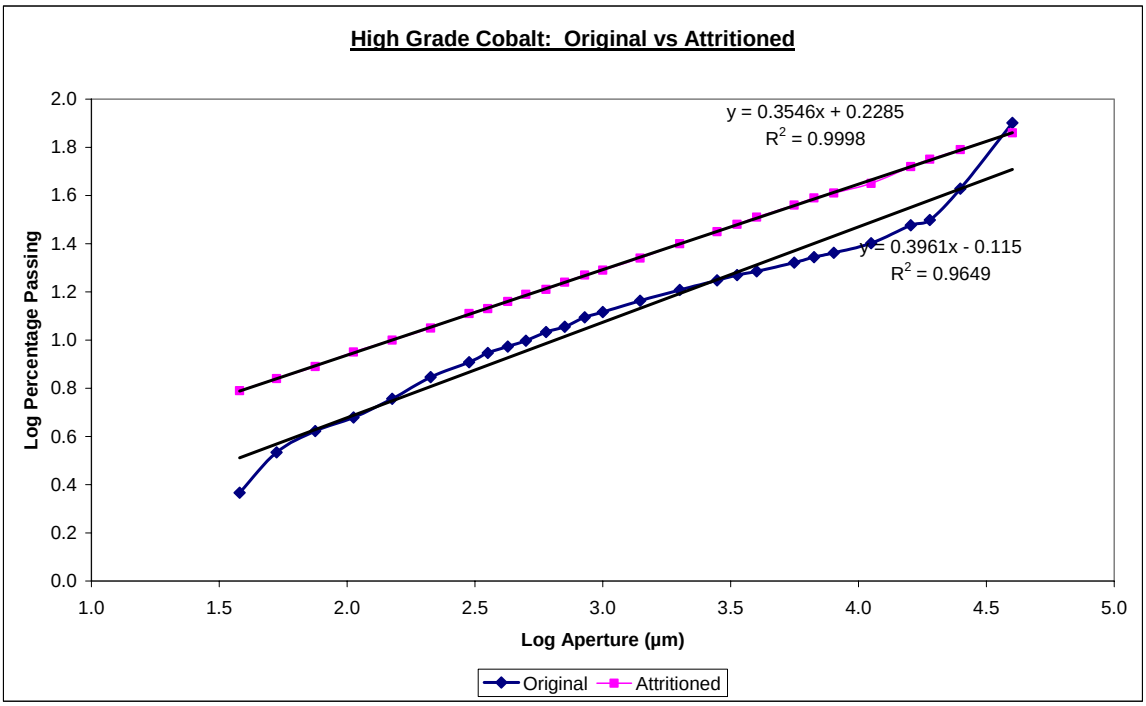

Figure 6: Paticle Size Distribution for original and attritioned material.

Coarse samples were selected for stereo-optical mineralogical examination and XRD analysis to identify the major minerals present. These were identified as heterogenite $Co_2O_3.H_2O$, malachite $Cu_2(CO_3)(OH)_2$, pecoraite $Ni_3SiO_5(OH)_4$ only minor quantities of gangue minerals were noted amongst which limonite $Fe_2O_3.3H_2O$ was identified. Such findings confirmed the high grade nature of the sample material. The coarse sample submitted for XRD examination were also analysed for their elemental content by means of AAS and XRF and the results are shown tables 10 to 14.

Table 10: XRF analysis of coarse high grade samples.

Sample	%Co	%Cu	%Ni	%Fe2o3	%Sio2	%Al2O3	%Fe(calc)
ATT	35.6	9.1	22.0	10.0	19.4	0.4	7.0
OR	56.3	10.0	11.1	7.8	8.6	1.1	5.5

Table 11: AAS analysis of coarse high grade samples

Sample	%Co	%Cu	%Ni	%Fe
ATT	32.1	6.9	13.4	3.7
OR	40.7	6.6	6.3	2.6

To determine the elemental distribution of values within the size ranges that might be anticipated in the products of a comminution process, representative aliquots from size range intervals for both the original sample and the attritioned product were analysed, this being by means of acid digestion and AAS analysis of the resultant solutions. From the residual solids an estimate a gravimetric estimate was made of the gangue content of the corresponding size intervals. These are shown in tables 12, 13 and 14.

Table 12: Analysis of fine fractions of original sample

Size µm	% Co	%Cu	%Fe	%Ni
-38	8.8	8.04	7.66	11.86
38	11.21	7.95	6.26	10.45
53	13.23	8.19	6.56	9.53
75	15.87	8.65	6.22	8.91
106	18.52	9.09	6.21	8.67
150	21.83	9.08	5.57	8.23
212	23.67	9.29	4.41	8
300	25.38	9.43	4.44	7.88
355	24.69	9.05	3.59	4.31
425	25.01	9.02	3.13	4.27
500	25.54	9.36	4.00	7.53
600	25.34	9.55	3.95	6.42
710	26.39	9.44	3.92	7.36
850	27.06	9.12	3.46	10.15
1000	26.03	9.63	4.10	5.81
1400	27.64	9.24	3.83	7.00

Table 13: Analysis of fines from attritioned material.

Size microns	% Co	%Cu	%Fe	%Ni
-38	13.43	12.74	6.37	9.49
38	17.6	12.73	6.97	7.12
53	19.82	13	7.13	6.55
75	20.52	13.43	7.16	6.27
106	23.08	13.84	6.28	5.87
150	25.72	13.91	4.87	5.45
212	26.82	13.66	4.44	5.55
300	29.44	14.5	4.25	7.09
355	29.65	14.55	3.57	7.43
425	31.28	13.47	3.65	7.13
500	30.12	12.97	3.40	7.19
600	31.02	12.23	2.78	6.67
710	32.31	11.71	2.91	6.33
850	33.15	10.31	3.98	6.92
1000	33.92	11.19	2.74	6.86
1400	34.68	10.03	2.92	6.72

Table 14: Acid insoluble residuals of fine fractions

Size microns	Original ore	Attritioned material
-38	30.47	19.69
38	30.16	15.88
53	25.58	13.16
75	19.55	9.51
106	15.65	9.05
150	12.92	7.93
212	10.82	7.53
300	9.55	7.5
355	9.88	7.17
425	9.65	6.39
500	10.43	6.18
600	9.87	6.37
710	9.78	6.56
850	7.78	6.02
1000	9.31	5.92
1400	7.57	5.29

From these analyses it is clear that the attritioning has had no major effect upon the value distribution of any of the elements analysed within the size ranges investigated. Also only two of the components show any trend relative to size variation, the cobalt value showing an increase with increasing particle size whilst the acid insolubles increase with decreasing size. These trends are even more evident when the data is presented in graphical format as in fig 11 for the acid insolubles and in figures 12 and 13 for the cobalt and other elements.

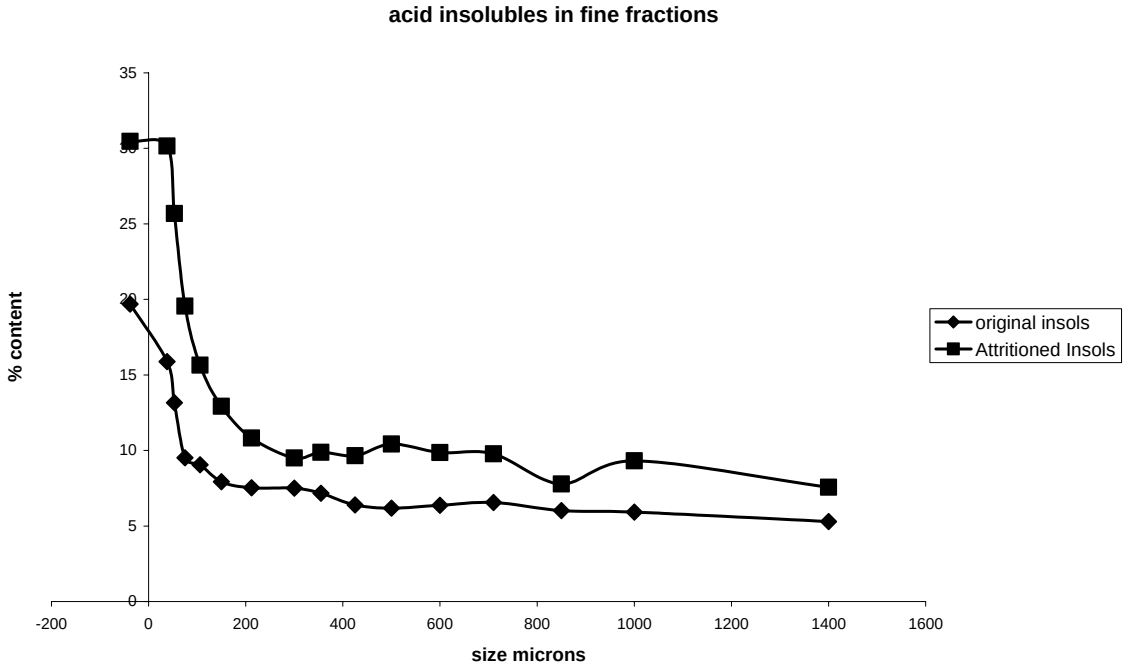

Figure 7: Acid insolubles versus size.

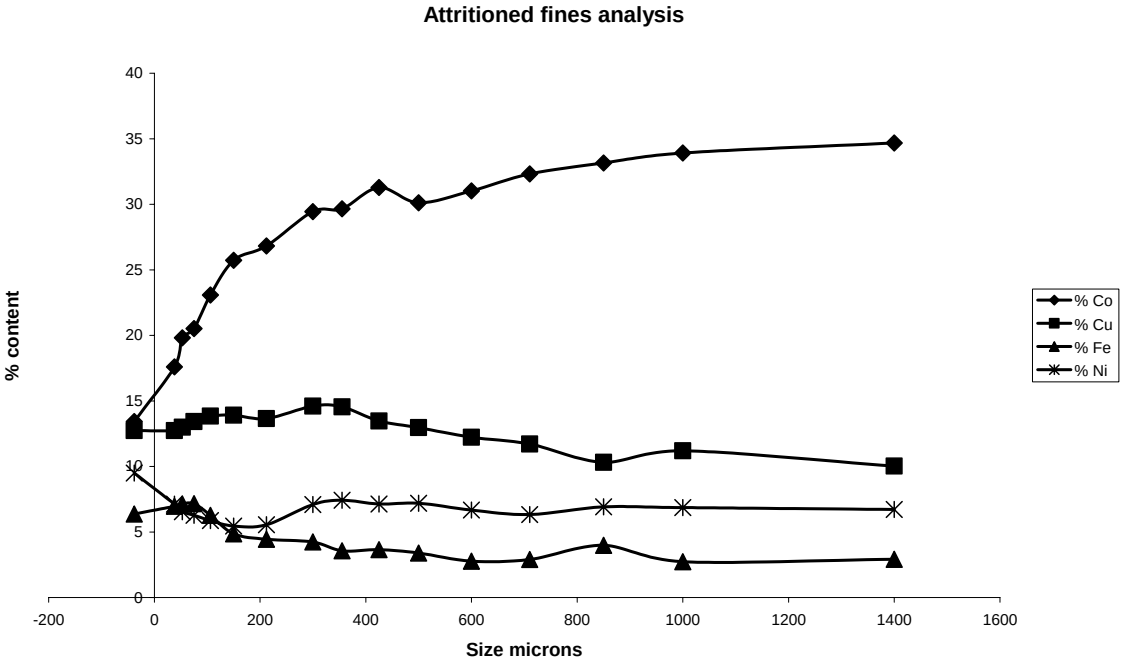

Figure 8: Attritioned fines analysis

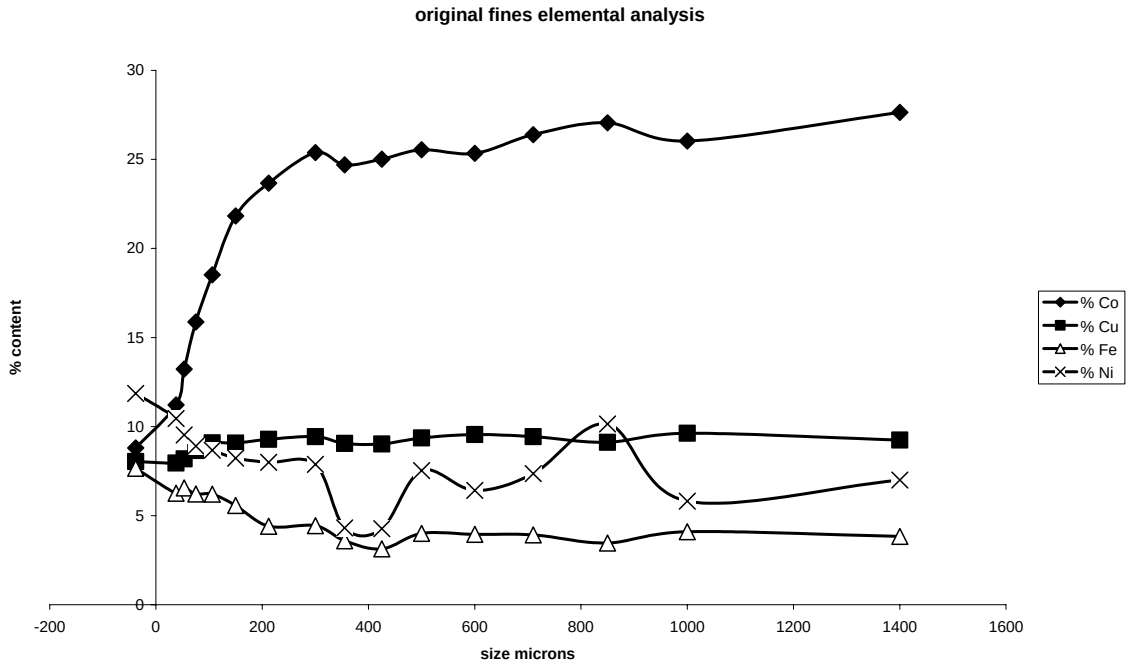

Figure 9: Original fines analysis

The form of the variation of the cobalt value with size suggests an approximation to a logarithmic expression and an attempt was made to fit this data to a logarithmic curve. The observed correlation coefficient corresponding was only 0.91 for the equation $y = -2.98x^{4.5}$ for the original sample material but when used to extrapolate to the size of the coarse particles analysed initially projected a value of 45% Co. In the case of the attritioned the correlation coefficient was 0.99 for an equation $y = 0.58x^{4.55}$ and extrapolated to a value of 53.4% Co. In a similar manner for the zinc bearing sulphide ore, selected size interval fractions were partitioned with the heavy liquid for both the original and attritioned materials. The mass partitioning results for this are shown in table 15.

Table 15: Mass partitioning of fine fractions.

	Original	Original	attritioned	Attritioned
Size mm	% Mass Float	% Mass sink	% Mass Float	% Mass sink
1.4	34.31	65.69	9.71	90.29
1	39.20	60.80	9.02	90.98
0.85	26.79	73.21	9.10	90.90
0.71	37.23	62.77	8.53	91.47
0.60	30.84	69.16	8.86	91.14
0.50	22.12	77.88	4.95	95.05
0.425	19.05	80.95	5.48	94.52
0.355	18.06	81.94	6.49	93.51
0.30	18.92	81.08	6.52	93.48

From these results it is evident that the simple attritioning of the coarse material has caused a major alteration in the mass partitioning on a density basis within all the size fraction interval examined. The low mass of the float fraction may be interpreted as a further indication of the high grade nature of the sample material. However as porosity may be present in these materials the presentation of density values against partitioning density is unlikely to be reliable and so the products were analysed for their base metal contents. The results are shown in the tables 16-18.

Table 16: Original TBE float fraction analyses

Size µm	% Co	% Cu	% Ni	% Fe	% insols.
>1400	24.60	8.31	7.62	5.02	14.87
>1000	24.84	9.11	4.91	5.97	16.4
..>850	23.46	8.42	5.23	6.01	19.08
>710	21.62	8.27	8.49	5.55	20.35
>600	22.02	8.30	5.40	5.98	20.83
>500	17.89	9.66	10.17	6.17	27.93
>425	10.18	4.94	4.56	4.20	27.59
>355	13.10	5.08	4.73	5.20	33.3
>300	15.50	5.64	8.02	5.36	28.83

Table 17: Original TBE sink fractions

Size µm	% Co	% Cu	% Ni	% Fe	% insols.
>1400	35.78	9.20	6.56	3.19	5.03
>1000	37.10	10.62	6.30	2.85	4.67
..>850	39.14	10.77	6.00	2.60	4.00
>710	36.45	10.13	6.77	2.98	4.90
>600	34.13	9.68	6.85	3.05	5.09
>500	33.88	9.99	6.99	3.44	5.84
>425	34.25	9.66	4.20	2.88	4.74
>355	33.02	9.62	4.22	3.24	3.94
>300	35.26	9.85	6.89	3.14	4.33

Table 18: Attritioned TBE float fractions

Size µm	% Co	% Cu	% Ni	% Fe	% insols.
>1400	25.69	7.49	7.39	3.99	17.44
>1000	21.26	8.64	5.44	4.94	21.53
..>850	19.30	10.03	5.99	5.52	22.80
>710	17.62	9.06	6.60	6.75	24.58
>600	16.52	9.07	6.15	5.46	26.19
>500	9.23	5.42	9.07	9.25	40.50
>425	13.44	7.27	8.40	4.78	34.16
>355	11.72	7.46	9.47	5.23	32.99
>300	10.77	6.34	9.10	4.61	38.22

Table 19: Attritioned TBE sink fractions

Size µm	% Co	% Cu	% Ni	% Fe	% insols.
>1400	36.26	9.04	6.65	2.81	3.38
>1000	35.00	11.40	6.35	2.55	4.11
..>850	34.20	12.10	6.30	2.25	4.15
>710	34.60	12.70	6.30	2.55	4.82
>600	34.10	12.81	6.30	2.65	4.31
>500	32.84	12.74	6.70	2.84	3.60
>425	31.80	13.66	7.24	3.62	4.34
>355	27.63	14.34	6.96	3.87	5.10
>300	30.11	14.35	7.31	4.25	5.30

Although there are significant elemental content differences between sink and float fractions within none of the size interval fractions is there any relatively barren material. This may be a consequence of the liberation size being below the size investigated or due to the porosity. When the irradiation with microwave energy is considered the same method was used as applied to the Black Mountain sample in that particles were exposed for varying times and the surface temperature measured. Results are shown in table 20.

Table 20: Response of high grade materials to irradiation.

sample	H2	H3	H12	H15	H24	H38	H50	H58	H62
Time sec	Deg C	Deg C	Deg C	Deg C	Deg C	Deg C	Deg C	Deg C	Deg C
30	182	156	100	127	94	112	131	156	91
60	234	200	187	160	183	183	178	212	176

Here it is clear that the sample material is responding as anticipated for the presence of high cobalt content. When the load versus displacement response of samples to compressive loading is examined the format of the results shows no indication of the

fracture observed in the Black Mountain material. A selection of results confirming this are shown in table 21.

Table 21: Load versus displacement for high grade cobalt samples.

Sample	H1	H10	H14	H12
Disp. Mm	Load kN	kN	kN	kN
0.635	0.28	0.28	0.28	0.28
1.27	0.46	0.28	0.28	0.28
1.905	0.32	0.28	0.28	0.98
2.54	0.84	0.46	0.28	1.49
3.175	0	0.28	0.74	1.53
3.81	0	0.42	0.98	1.81
4.445	0	0.37	1.21	1.72
5.08	0	0.28	1.53	2.28
5.715	0	0.42	1.67	1.67
6.35	0	0.32	1.67	1.39
6.985	0.19	0.85	1.91	1.39
7.62	0	0.65	2.79	2.09
8.255	0	0.93	3.25	1.53
8.89	0.14	1.35	4.14	2.09
9.525.	0	1.3	5.39	2.74

The sizing analysis of the products is shown in table 22. The only significant difference observed in the + 11.2 mm fractions between samples H14 and H12 which were exposed to microwave irradiation prior to the test unlike H1 & h10 which were not.

Table 22: Size analysis of products from compression test.

Sample	H1	H10	H14	H12
Density	1.62	2.28	2.82	2.5
Size	% mass	% mass	% mass	% mass
11.2	49.1	32.7	5.1	7.6
8	5.9	2	8.2	18.7
5.6	2.5	10	10.7	13.6
4	4.3	8.9	13.1	8
1.4	6.5	15.4	22.7	17.6
1	2.2	3.6	5.3	5.1
-1	29.6	27.4	34.9	29.5

5. Conclusions and recommendations.

Both sample materials were shown to be heated by the microwave energy even at the low power levels of the microwave oven (900 W). The high cobalt sample responding more effectively than the sulphide. When the fracture under compression is examined all the zinc sulphide ore materials showed similar characteristics, whilst the high cobalt oxide sample gives no indication of such structural failure.
Examination of the products from heavy liquid partitioning shows that the zinc sulfide material has a tendency to release gangue components from the particle matrix even without microwave irradiation. No indication of a favourable response to value liberation has been observed for the high grade cobalt oxide materials. It is also recognized that the use of the heavy liquid method of assessment may not be appropriate to this sample as a consequence of the identified particle porosity.

The hand picked high grade cobalt oxide sample having very little gangue content has no requirement for any enhancement of value liberation and is of such a physical composition that knowledge gained from its examination is unlikely to be valid for cobalt oxide ores of a more conventional composition (1-3%Co) and structure. However in view of the known and demonstrated response of the cobalt mineral to the microwave heating an ore of more realistic composition should be tested.

The zinc sulphide ore material on the other hand already shows potential for liberation which it is anticipated can be enhanced with the use of microwaves. The present results show that the techniques applied in this investigation yield indicators relative to mineral liberation.

It is suggested that the work on the zinc sulphide ore continues and that the techniques developed be tested upon other ore samples as a means of preliminary assessment of microwave potential applications.

6. References.

Beck, R.D., and Chamart, J.J., (1980). The Broken Hill Concentrator of Black Mountain Mineral development Company (Pty) Limited South Africa, The South African Institute of Mining and Metallurgy, Conference on Complex Sulphide ores, Oct. 1980. pp 88-99.

Bradshaw S.M., (1999).Applications of Microwave heating in mineral processing, South African Journal of Science 95, September 1999, pp 394 – 396.

Fandrich R.G., Bearman R.A., Boland J., Lim W., (1997). Mineral Liberation by Particle Bed breakage, Minerals Engineering, vol 10, No 2, pp 175 – 187, 1997.

Güngor A., Atalay Ü., (1998). Microwave processing and grindability, 7th Int. Min. Proc. Symp. (comminution, classification and sizing) Istambul 1998, pp13 – 16.

Kanellopoulous A., Ball A., (1975). The fracture and thermal weakening of quartzite in relation to comminution, JSAIMM, vol 76, Oct 75, pp45 – 52.

Kingman S.W., Vorster W., Rowson N.A., (2000). The effect of microwave radiation on the processing of Palabora Copper ore, JSAIMM., vol 100, No 3, May/June 2000, pp 197 – 204.

Kingman S.W., Vorster W., Rowson N.A., (2000). The influence of mineralogy on microwave assisted grinding, Minerals Engineering, vol 13, No 3, pp 313 – 327.

Lewis, J, (2005), An investigation on Microwave assisted comminution, M-Tech dissertation, University of Johannesburg.

Patnaik N., Rao R.B., (2004). Microwave Energy in Mineral Processing – A Review, IE (I) Jornal – MN, Vol 84, February 2004, pp 56 – 61.